

SYNTHESIS AND ELECTROCHEMICAL CHARACTERIZATION OF Li_3PO_4 FOR SOLID STATE ELECTROLYTES

H. Jodi^{1,2}, Supardi¹, E. Kartini¹ and Anne Zulfia²

¹Center for Science and Technology of Advanced Materials - BATAN

Kawasan Puspiptek, Serpong 15314, Tangerang Selatan

²Department of Metallurgy and Materials Engineering, Faculty of Engineering - UI

Kampus UI Depok, Jawa Barat 16424

E-mail: heriendi@batan.go.id

Received: 15 December 2015

Revised: 4 July 2016

Accepted: 19 September 2016

ABSTRACT

SYNTHESIS AND ELECTROCHEMICAL CHARACTERIZATION OF Li_3PO_4 FOR SOLID STATE ELECTROLYTES. The application of solid state electrolytes to solid state battery becomes important research area, recently, to overcome leakage and combustion issues involved in liquid electrolytes. Solid state electrolytes are safer, easily packaged and have several advantages, including easy fabrication, high ionic conductivity at room temperature and wide compositional range. Here in this study we characterized Li_3PO_4 for solid state electrolyte, synthesized by solid state reaction and wet chemical reaction methods. The samples were characterized using Electrochemical Impedance Spectrometer (EIS) to determine its electrical properties in addition to X-Ray Diffraction and Scanning Electron Microscope -Energy Dispersive X-Rays Spectroscopy (SEM-EDS) characterizations. Both of samples that have been characterized have a high electrical resistivity on the order of tens MW, with DC conductivity in order of 10^{-10} to 10^{-9} S/cm.

Keywords: Li_3PO_4 , Solid state Electrolytes, EIS, Dielectric constant, Conductivity

ABSTRAK

SINTESIS DAN KARAKTERISASI ELEKTROKIMIA Li_3PO_4 UNTUK ELEKTROLIT PADAT. Penggunaan elektrolit bentuk padat pada baterai menjadi sebuah area riset yang penting untuk menghadapi isu masalah kebocoran dan kebakaran baterai yang diakibatkan penggunaan elektrolit jenis cair. Selain lebih aman dan kemudahan dalam pengemasan, elektrolit bentuk padat relatif mudah pembuatannya, titik cairnya rendah, memiliki konduktivitas ionik yang tinggi dalam suhu kamar dan rentang komposisi pembuatan yang lebar. Pada penelitian ini telah dilakukan karakterisasi Li_3PO_4 untuk elektrolit padat yang didapatkan melalui sintesis menggunakan Metode Reaksi Padatan dan Metode Reaksi Kimia Basah. Sampel yang dihasilkan dari sintesis tersebut dikarakterisasi menggunakan *Electrochemical Impedance Spectrometer (EIS)* untuk mengetahui sifat kelistrikannya ditambahkan pada hasil karakterisasi menggunakan *X-Ray Diffractometer (XRD)* dan *Spectrometer Electron Microscope - Energy Disphre Spectroscopy (SEM-EDS)*. Kedua sampel hasil sintesis tersebut memiliki tahanan listrik yang tinggi dalam orde MW, dan memiliki konduktivitas listrik dalam rentang orde 10^{-10} hingga 10^{-9} S/cm.

Kata kunci: Li_3PO_4 , Elektrolit padat, EIS, Konstanta dielektrik, Konduktivitas

INTRODUCTION

Increased use of electronic goods and the demand for hybrid technologies require to be followed by research and discovery of the battery as a very important power source such as Lithium-based batteries as a sample of power source provide great energy due to oxidation of the very high energy with a relatively small mass of Lithium inside.

In general, electrolyte of a battery consists of a solution of lithium salt dissolved in an organic solvent. It will cause an irreversible loss of battery capacity, which could not be recovered as a result of the formation of a stable layer between the electrodes and the electrolyte or often called the Solid Electrolyte Interphase (SEI). In addition to the reaction between the electrolyte and the electrodes, the use of liquid electrolyte types also inhibits the increase in the life cycle of batteries, limiting the battery usage temperature range, difficult to miniaturization, causing leakage and security issues, etc. Because of these problems, the replacement of the liquid electrolyte that has been used, with the solid electrolyte is an issue that is interesting and quite urgent to do.

Solid type electrolyte is very interesting because of its potential to be applied in a wide variety of electrochemical devices such as batteries solid (solid state battery), sensors, timers, fuel cells, memory, capacitors etc. And because of the dense, solid electrolyte is expected to unravel the problems associated with a loss of capacity, the time of life, security and temperature ranges as described above [1,2]. Solid electrolyte has an advantage in terms of ease of design, does not cause leakage and pollution and has a better resistance to shock and vibration compared to liquid electrolytes [3]. Solid electrolyte is also a single ion conductor which means only one type of carrier are shipped in a solid electrolyte. As a result, an ionic conductor can have ionic transfer number close to one. Therefore, during the operation, there is almost no concentration gradient in the cell. It is very advantageous to reduce the potential of cell over-potential [4].

Solid electrolyte based on glass material made a lot of attention because their advantages over crystalline solid electrolyte one. These advantages include the isotropic ion conduction, the absence of grain boundary resistance, wide range of composition of the glass former, easy in preparation, easy forming, inert to the environment, etc. In addition, the amorphous glass materials generally have a higher ionic conductivity than the crystalline solid electrolyte material. That is because the glass based solid electrolyte material is believed to have an open structure or greater free space (open space). Electronic conductivity in the glasses can be ignored, so electronic leakage in device that uses solid electrolytes can be avoided.

Lithium Phosphate (Li_3PO_4) is one of the best glassy solid electrolytes ever made. However, this material possesses low enough conductivity to be applied to a battery, because it has a large bulk resistance. Therefore Li_3PO_4 solid electrolyte materials are widely used as the electrolyte in the battery in the form of a thin layer to reduce the resistance value. Solid electrolyte based Phosphate Oxide materials are ease of preparation, strong glass forming character, low melting points and simple composition. Previous research have proposed Phosphate Oxide based material as a solid state electrolyte [5,6].

The crystal structures of Li_3PO_4 are derived from wurtzite and are built up of Oxygens in approximately hexagonal close packing which the lithium and Phosphorus cations ordered over one set of tetrahedral sites. There are three stable polymorphs of Li_3PO_4 that called α , β and γ - Li_3PO_4 . α -form is stable in a short range below melting point. γ -form kinetically stable to room temperature but thermodynamically stable form under 40 °C β - Li_3PO_4 . The transition of $\beta \rightarrow \gamma$ - Li_3PO_4 is about 400-580 °C and the transition is irreversible. Reversible transition from $\gamma \rightarrow \alpha$ and α - $\text{Li}_3\text{PO}_4 \rightarrow$ liquid phase occurred near 118 °C and 122 °C respectively [7]. Investigations on the structures, detailed atomistic Li^+ ion diffusion mechanisms and mobility in idealized Li_3PO_4 crystals and related phosphorus electrolytes based on Li_3PO_4 have previously been reported in works involving first-principles modeling techniques [8-10]. In those materials Lithium ion can diffuse with relatively low migration energy of 0.3-0.7 eV by vacancy or interstitial mechanisms.

Glass materials such as Li_3PO_4 are commonly synthesized using Solid State Reaction technique, by heating glass former materials to above their melting point and cooling rapidly (melt-quenching method) to obtain desired glass phases. To get a good glass phase required a very fast cooling rate. When the cooling rate is not sufficient then the resulting material becomes a combination of glass and crystalline. The glass material have to prepared by very fast cooling rate technique such as twin roller rapid quenching technique that can quench at ratio of 10^6 K/s to avoid crystallization.

Many works of research on the Li_3PO_4 ionic conductors have been reported, but none that present discussion on the relationships between the synthesis methods and electrochemical properties of Li_3PO_4 . Similar works were reported on discussion on relationships between synthesize methods and structural and morphological characterization [11,12]. Another work were reported structural analysis of the electrolytes using High Resolution Neutron Diffraction method [13]. This study is focused on electrochemical characterization to characterize Li_3PO_4 obtained by two techniques called Solid state reaction (SSR) and Wet chemical reaction (WCR) technique. Synthesized samples were characterized using X-Ray Diffraction, SEM-EDS as well

as the electrical properties using Electrochemical Impedance Spectrometry. The results are then compared to see the electrochemical properties of the samples in conjunction with synthesis methods. Wet chemical reaction technique is easier and does not require high temperature heating. This technique could also provide more Li_3PO_4 material in a single process. Solid state reaction in other hand, need heating to a certain high temperature and rapid cooling. WCR technique gave more pure and homogenous Li_3PO_4 , but the conductivity was lower than the conductivity of samples prepared by SSR technique.

EXPERIMENTAL METHOD

Materials and Tools

The samples for this work are prepared simultaneously with the samples for the group in previous work [12]. Starting materials used as precursors of Li_3PO_4 were LiOH (Merck, 98%) and H_3PO_4 (Merck, 98%) for wet chemical reaction technique, Li_2CO_3 (Alfa Caesar, 99%) and $\text{NH}_4\text{H}_2\text{PO}_4$ (Merck, 98%) for solid state reaction technique. Patri dishes, baker glasses, magnetic stirrer and demineralized water were used as aids for wet chemical reaction, ceramics crucibles, mortar and pestle, heating furnace and liquid Nitrogen were used for solid state reaction.

Shimadzu XD-610 X-Ray Diffractometer with a scintillation counter was carried to record the X-ray diffraction pattern of the samples. The XRD equipped with a Ni filtered source target $\text{Cu K}_{\alpha 1}$ sealed X-ray tube ($\lambda=0.1540598 \text{ \AA}$), 45 kV applied voltage and 40 mA current, 1° source slit and 0.6 mm receiving slit. Patterns were recorded over goniometer (2θ) from $5-100^\circ$ in a STEP scan mode, with a step size of 0.02° . Spectral data were analyzed using HighScore Plus ver. 3.0e from PANalytical which licensed to Badan Tenaga Nuklir Nasional.

JEOL JSM-6510LA Scanning Electron Microscopy (SEM) equipped with Energy Dispersive X-Ray Spectroscopy (EDS) was utilized to observe the cross-sectional view (morphology) of the samples. The SEM was operating at 20kV, a chamber pressure of 20 Pa, wide distance of 10 mm and Spot Size of 65. The EDS was used for elemental analysis or chemical characterization of the samples. AC Impedance Measurement of Li_3PO_4 samples were carried out using HIOKI LCR HiTester 3532-50. Silver paste was attached to Li_3PO_4 pallets, serving as ion-blocking electrodes. Impedance spectra were collected in an ambient atmosphere and temperature, at applied voltage of 1 V, over a frequency range of 42 Hz- 5 MHz.

Experimental Procedure

In wet chemical reaction technique, 1M LiOH and 1M H_3PO_4 were mixed with molar ratio of 3:1 in

demineralized water using magnetic stirrer for 5 hours at 40°C . The products of this reaction were precipitated Li_3PO_4 and water. After washing process, separated Li_3PO_4 was dried at 110°C for 7 hours and grounded for an hour by hand mill.

For solid state reaction, Li_2CO_3 and $\text{NH}_4\text{H}_2\text{PO}_4$ were mixed at molar ratio of 3:2 and ground together in a crucible for an hour. The mixture was then gradually heated from 200°C , 400°C , 675°C and 775°C for several hours. The molten mixture was quenched into liquid Nitrogen and smoothed by hand mill for an hour.

The samples are then characterized by XRD and SEM/EDS characterization. For electrochemical characterization, powder samples were palletted with pressure of 5000 psi. Both surfaces of the palletes were coated by Ag paste that serve as ion blocking electrode and current collector.

All of the activities of synthesis and characterizations were being done at The Integrated Battery Laboratory, Center for Science and Technology of Advanced Materials, Indonesian National Nuclear Energy Agency.

RESULTS AND DISCUSSION

XRD spectra for the Li_3PO_4 obtained by Wet Chemical Reaction (WCR) are shown in Figure 1 (a) and by Solid State Reaction (SSR) are shown in Figure 1 (b). The results show both of the spectra was combination of crystalline spectra and amorphous spectra. The results also indicated that both samples were composed mainly of Li_3PO_4 crystals.

The spectral XRD data pattern from Li_3PO_4 obtained by wet chemical reaction were matched with the standard Li_3PO_4 (Reference Code #96-901-2501) and shown that they had similar pattern, that indicated that our Li_3PO_4 samples had quite good quality. The crystal structure matched to the orthorhombic structure with

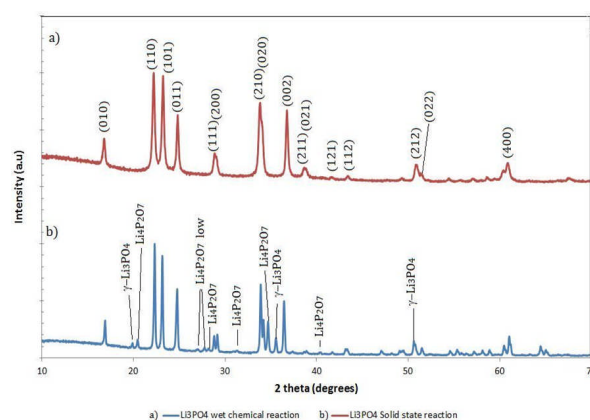


Figure 1. X-Ray Diffraction (XRD) pattern of Li_3PO_4 samples produced by (a). WCR - Wet Chemical Reaction Method and (b). SSR - Solid State Reaction Method. The spectral data indicated that both samples were composed mainly of Li_3PO_4 crystal, same as published by previous work [12].

space group of $P m n 2_1$ (#31). The formation of Li_3PO_4 by Wet chemical reaction occurs at lower temperature below transition of $\beta \rightarrow \gamma$ phase. According to previous references, the crystal structure of this XRD pattern belongs to $\beta\text{-Li}_3\text{PO}_4$ phase [7-9].

In the solid state reaction sample the amount of matched Li_3PO_4 phase was about 86%. The crystal structure matched to the orthorhombic structure of Li_3PO_4 with Reference code #00-015-0760, space group of $P m n b$ (#62). The formation of Li_3PO_4 on solid state reaction occurs at higher temperature below transition of $\beta \rightarrow \gamma$ phase. As shown in Figure 1(b) the spectral data contain some peaks of phases denoted by $\gamma\text{-Li}_3\text{PO}_4$ which means those peaks are purely belong to $\gamma\text{-Li}_3\text{PO}_4$ phase. The other peaks are concurrent reflections of both $\gamma\text{-Li}_3\text{PO}_4$ and $\beta\text{-Li}_3\text{PO}_4$. The formation of $\gamma\text{-Li}_3\text{PO}_4$ is due to heating treatment applied to the sample above their $\beta \rightarrow \gamma$ transition temperature and in this our case the applied temperature is up to 775°C that enough to transform the β to γ phases. This heat treatment affects the length and strength of the bonds, which resulted in the expansion of the crystal structure of the $\beta\text{-Li}_3\text{PO}_4$ and transform to $\gamma\text{-Li}_3\text{PO}_4$ [7]. The transition of $\beta \rightarrow \gamma\text{-Li}_3\text{PO}_4$ is irreversible transition, in consequence, there were no possibilities for $\beta\text{-Li}_3\text{PO}_4$ phase to be formed back. So it can be concluded that this XRD pattern belong to crystal structure of $\gamma\text{-Li}_3\text{PO}_4$ phase. These results of $\beta\text{-Li}_3\text{PO}_4$ in wet chemical reaction and $\gamma\text{-Li}_3\text{PO}_4$ in solid state reaction were confirmed by analysis using Rietveld Refinement of XRD spectral data [12].

Another peaks that indicated as impurities in the spectral data belong to $\text{Li}_4\text{P}_2\text{O}_7$ crystal. $\text{Li}_4\text{P}_2\text{O}_7$ has two polymorphs, anorthic (P -1) at low temperature and monoclinic (P 1 21/n 1) at high temperature. The transition temperature is about 610-613 °C [14]. The peaks of monoclinic $\text{Li}_4\text{P}_2\text{O}_7$ (high T) patterns are in the same position with those of anorthic one and of the orthorhombic Li_3PO_4 . Hence no peaks that are purely owned by monoclinic form can be found. But there were two peaks found to be owned by anorthic form (low T) that in Figure 1 (b) denoted as $\text{Li}_4\text{P}_2\text{O}_7$ low. More than that, $\text{Li}_4\text{P}_2\text{O}_7$ compound has a reversible heat effect during heating at its transition temperature that confirmed a fast and reversible polymorphic inversion.

Therefore, the high form of monoclinic $\text{Li}_4\text{P}_2\text{O}_7$ could not be obtained at room temperature by quenching. Even when the melt of $\text{Li}_4\text{P}_2\text{O}_7$ is quenched from above the melting point, the $\text{Li}_4\text{P}_2\text{O}_7$ crystals are always the low temperature form (anorthic). These facts indicated that the diffraction pattern of the $\text{Li}_4\text{P}_2\text{O}_7$ on this solid state reaction sample belong to the low temperature form of anorthic $\text{Li}_4\text{P}_2\text{O}_7$. It's peaks were in agree with standard $\text{Li}_4\text{P}_2\text{O}_7$ in database #98-005-9243. The formation of $\text{Li}_4\text{P}_2\text{O}_7$ in this case may be caused by inhomogeneous mixing of the sample that result in different ratio of mixture of precursors Li_2O and P_2O_5 upon heating [6]. The

Table 1. Composition and crystal system of phases contained in the samples, obtained from X-ray Diffraction Data Analysis. The Crystal parameters were obtained from database with Reference Code No. 96-901-2501, 00-015-0760 and 98-005-9243

Method	WCR		SSR
Formula	Li_3PO_4 (β)	Li_3PO_4 (γ)	$\text{Li}_4\text{P}_2\text{O}_7$
Space group	$P m n 2_1$ (31)	$P m n b$ (62)	$P -1$ (2)
Crystal system	orthorhombic	orthorhombic	anorthic
Unit cell	a= 6.1150 Å	a= 6.1147 Å	a= 5.1850 Å
	b= 5.2390 Å	b= 10.4750 Å	b= 7.1052 Å
	c= 4.8550 Å	c= 4.9228 Å	c= 8.5610 Å
	$\alpha = \beta = \gamma = 90^\circ$	$\alpha = \beta = \gamma = 90^\circ$	$\alpha = 103.0630^\circ$ $\beta = 90.0140^\circ$ $\gamma = 111.3430^\circ$

composition and structure of each phase from XRD analysis are resumed in Table 1.

Figure 2 shows the micrographs of Li_3PO_4 samples obtained from wet chemical reaction and solid state reaction. No clear morphological differences have been observed of these micrographs, but the sample of wet chemical reaction more homogeneously dispersed. Agglomeration of particles is observed in both samples indicating that the actual size of the particles may be even smaller than size observed in these micrographs. The particle size of the Li_3PO_4 powder obtained by wet chemical reaction is about 0.7-7.8 μm meanwhile powder from solid state reaction is about 2.2-17.3 μm . That's mean that the powder from wet chemical reaction is more homogeneous. The homogeneity of this sample is due to the fact that the sample consists of almost pure Li_3PO_4 as discussed before. The agglomeration in the sample of wet chemical reaction may due to slightly excess of precursor LiOH from the reaction. The agglomeration in the solid state reaction sample is observed more exist and larger than that of wet chemical reaction sample. This is may occur as results of the gradually heating conducted to the sample during the synthesis. This slow heating can form $\text{Li}_4\text{P}_2\text{O}_7$ compound which other

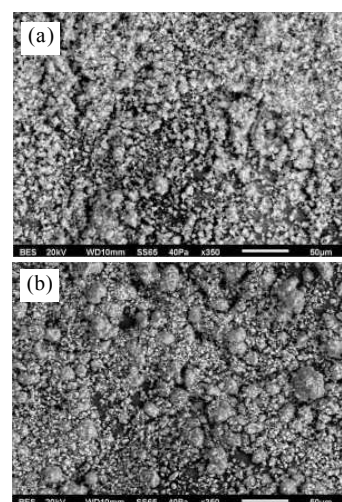


Figure 2. Scanning Electron Microscope (SEM) of Li_3PO_4 samples produced by (a). Wet Chemical Reaction and (b). Solid State Reaction.

polymorph of $\text{Li}_2\text{O-P}_2\text{O}_5$ system that melted below the highest temperature of the reaction.

Quantitative analysis with EDS give area elemental composition of these samples which dominated by element of O and P. For Li_3PO_4 prepared by Solid State Reaction the ratio atomic composition of O to P is 4.01. It is mean that the area elemental composition almost consisted of element P and O with ratio of 1:4 which means that in average the sample are dominated by Li_3PO_4 .

For the Li_3PO_4 prepared by wet chemical reaction, the ratio atomic composition of O to P is 8.61. It's mean that beside of Li_3PO_4 in this area also consist of other elements which their value counted to the percentage of O. These elements must be in a small amount and consist of O or elements that smaller than Beryllium which is used as cover guard of SEM detector. X-ray energy from elements smaller than Be (i.e. Li and H) will be absorbed by the Beryllium before reaching the detector. Therefore, they could not be detected by the analyzer, and their energy will be counted to the nearest element in the EDS observation. In this case the nearest element is O, so the energy from Li and H will be calculated as energy from O. As discussed before, the Wet chemical reaction sample may also consist of excess LiOH from reaction that form agglomeration with Li_3PO_4 particles. All of the atomic percentage of this LiOH elements may be counted to value of element O which resulted in a big ratio of O to P in this sample. Detailed discussion of the morphology of Li_3PO_4 also can be found in the work by Prayogi et.al. [11].

The shape of Impedance spectra of Li_3PO_4 obtained from wet chemical reaction and solid state reaction, shown in Figure 3. The spectra were obtained from the range frequency of $f = 42 \text{ Hz} - 5 \text{ MHz}$. There were no clear semicircle loops observed in both spectra.

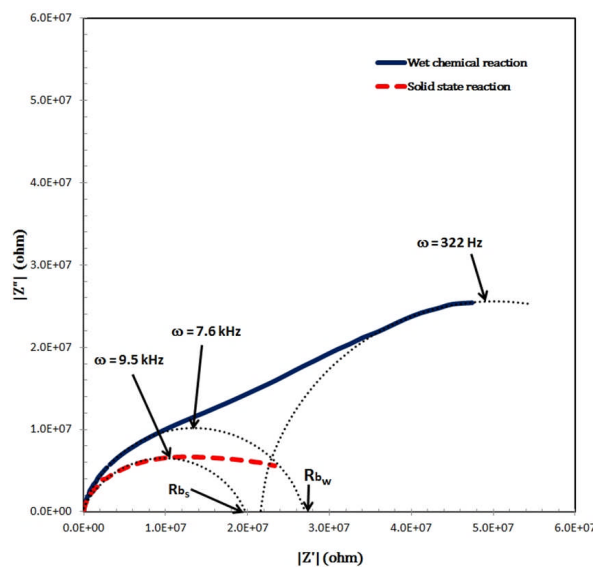


Figure 3. Impedance Spectra Diagram (Nyquist Plot) for Li_3PO_4 samples produced by Solid State Reaction (dark line) and Wet Chemical Reaction (red line).

Impedance diagram of sample prepared by wet chemical reaction appears to consist of two capacitive loops with two capacitive time constant. A semicircle could be analogous to an electrical circuit consisting of a resistor and a capacitor in parallel connection. Distorted and depressed semicircles may arise due to overlap of semicircles with various time constants, properties of the electrolyte not being homogenous, distributed microscopic properties of the electrolyte, etc.

Inspection of the data reveal that the relaxation frequency for this sample, i.e. the frequency which has the highest capacitive impedance value in the loop on investigation, were $(\omega = 2\pi f)_{\max} = 7.570 \text{ kHz}$ for the first loop in the higher frequency range, and $\omega = 322 \text{ Hz}$ for the second capacitive loop in the lower frequency range. So the relaxation time $(\tau = 1/\omega)$ are $\tau = 1.32 \times 10^{-4} \text{ s}$ for the first loop and $\tau = 3.11 \times 10^{-3} \text{ s}$ for the second one. The first loop give resistance value of $R_{b_w} = 2.77 \times 10^7 \Omega$ and capacitance of $C_{b_w} = 4.77 \times 10^{-12} \text{ F}$ is in the higher frequency region that in this observation can be interpreted as response of the bulk to the electric field. For the second loop the value were $R = 5.76 \times 10^7 \Omega$ and $C = 5.39 \times 10^{-12} \text{ F}$ is in lower frequency region, and can be interpreted as response from grain boundary in the sample.

A depressed loop in the complex impedance plane for Li_3PO_4 prepared by Solid State Reaction sample was observed and gave one semicircle with one relaxation time. The relaxation frequency is $\omega = 9.5 \text{ kHz}$, so the relaxation time is $\tau = 1.06 \times 10^{-4} \text{ s}$. The bulk resistance capacitance of the sample are $R_{b_s} = 1.98 \times 10^7 \Omega$ and $C = 5.36 \times 10^{-12} \text{ F}$. Table 2 give resume of these impedance values obtained from Figure 3 of Impedance Spectra Diagram.

Table 2. Impedance values obtained from the impedance spectra diagram of Li_3PO_4 samples prepared by solid state reaction and wet chemical reaction.

Preparation method	WCR		SSR
	Loop1	Loop2	Loop1
Relaxation frequency (Hz)	7570.42	322.06	9455.56
Relaxation time (s)	1.32×10^{-4}	3.11×10^{-3}	1.06×10^{-4}
Resistance (ohm)	2.77×10^7	5.76×10^7	1.98×10^7
Capasiance (F)	4.77×10^{-12}	5.39×10^{-11}	5.36×10^{-12}

Figure 4 shows the Bode plot for Li_3PO_4 samples prepared by Wet Chemical Reaction and Solid State Reaction. The resistive Impedance of WCR and SSR samples have a same tendency curve as showed by Figure 4 (a). Start from high frequency the pattern make a plateau area and then increase while frequency is decreasing. Only the impedance value were different at low frequency, that is the impedance of SSR sample is lower than that for the WCR sample.

For the imaginary part of the impedance as showed by Figure 4 (b) the patterns show a different tendency. While for the SSR sample the capacitive impedance tends to decrease at low frequency, the capacitive impedance for WCR samples were increased

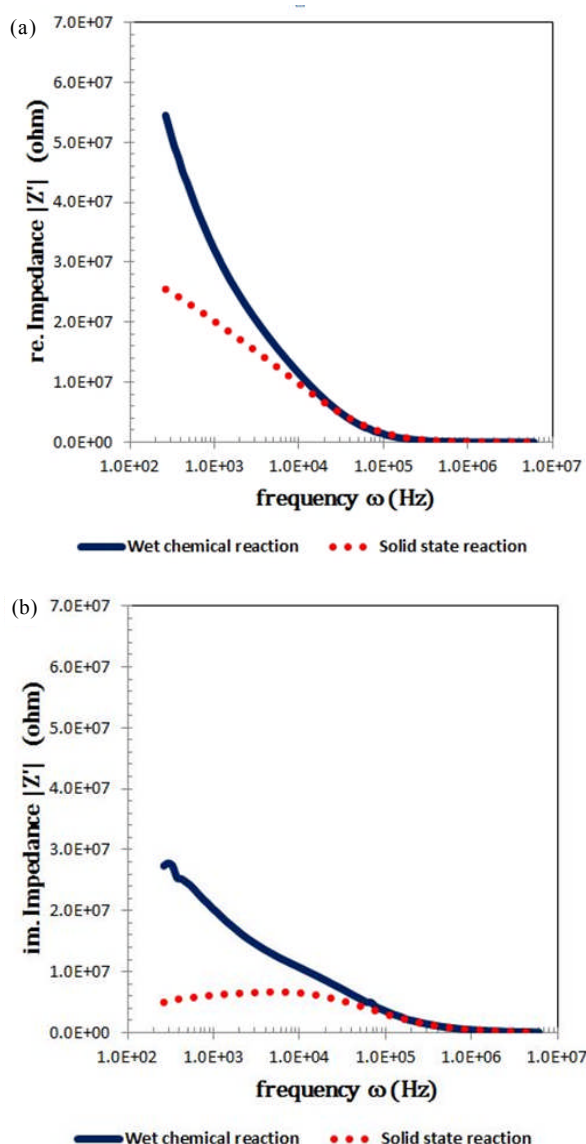


Figure 4. The Bode plot for Li_3PO_4 sample prepared by Solid State Reaction and Wet Chemical Reaction. (a). Resistive Impedance Plot, and (b). Capacitive Impedance Plot.

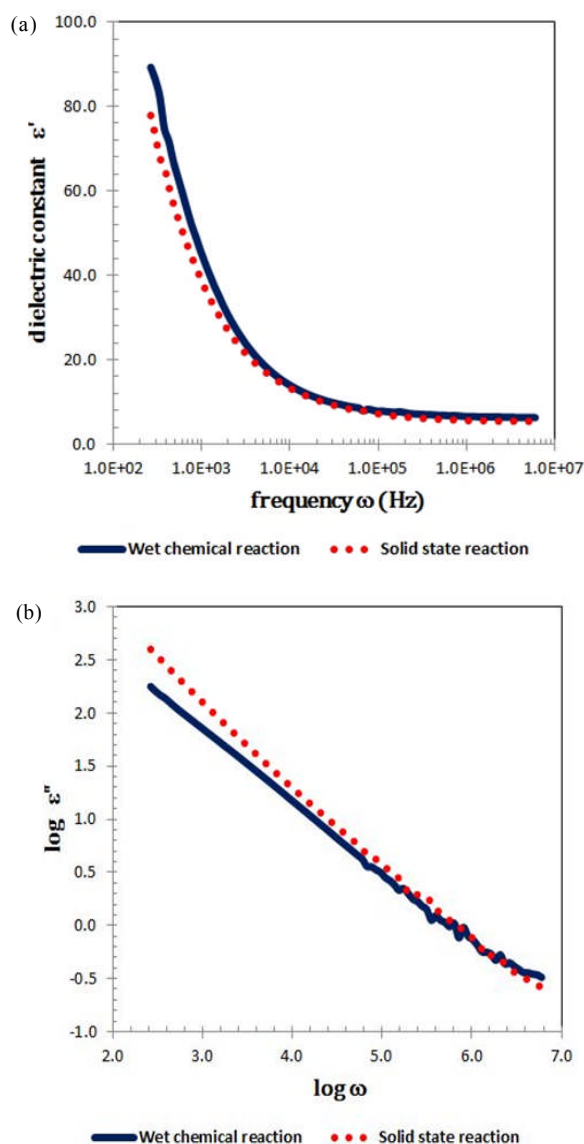


Figure 5. Frequency dependent plots of permittivity for Li_3PO_4 samples prepared by Solid State Reaction and Wet Chemical Reaction. (a). Dielectric constant Plot, and (b). Dielectric loss Plot.

and look like to make second peak at lower frequency. This difference of capacitive impedance characteristics confirmed the pattern of Nyquist plot (Figure 3) of these samples were different at the same frequency range with the appearance of the second loop. So we can conclude that the difference of impedance pattern of these samples is due to the difference response of capacitive impedance in the low frequency range. The study of dielectric properties is essential to gain information about loss of energy mechanism. Figure 5 show the plot of the frequency dependent of permittivity of Li_3PO_4 samples. The parameters were calculated from the real and imaginary part of the impedance. The dielectric constant is the real part of Complex permittivity parameter that can be expressed as:

$$\epsilon^* = \epsilon' - j\epsilon'' = (j\omega C_0 Z^*)^{-1} \quad (1)$$

where j , ω , C_0 and Z^* refer to imaginary unit, angular frequency, vacuum dielectric permittivity constant and the complex impedance respectively. The real part of permittivity is lossless dielectric or dielectric constant, and the imaginary part is dielectric loss.

As showed by Figure 5.a), the dielectric constant curve of Li_3PO_4 prepared by Wet chemical Reaction in the range of measurable frequency is stuck together with that for Li_3PO_4 prepared by Solid state reaction. In the low frequency range, a strong frequency dispersion of permittivity is observed. It's followed by nearly frequency independent behavior and attains a constant limiting value that can be attributed to free dipoles vibrations in an AC fields[15].

Just at the low frequency, the value of dielectric constant of the SSR sample take a little bit lower than

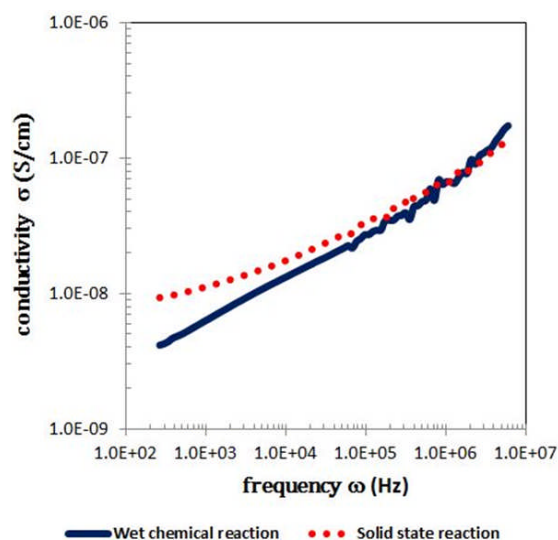
Table 3. List of dielectric constant, dielectric loss and tandelta value of Li_3PO_4 samples in several frequencies

frequency	WCR			SSR		
	60 Hz	10 kHz	1 MHz	60 Hz	10 kHz	1 MHz
Dielectric constant	74.8	7.91	6.27	65.8	7.92	5.39
Dielectric loss	139.5	3.60	0.33	290.8	4.57	0.26
Dielectric loss slope		-0.654			-0.733	
Tandelta	1.87	0.46	0.05	4.42	0.06	0.05

that for WCR sample. It means that both of the preparation methods produce Li_3PO_4 powder which have same dielectric lossless characteristic, even amount of Li_3PO_4 in the sample of SSR some fewer than that of WCR. At point of frequency $\omega = 10$ kHz, the value of dielectric constant of these samples were 7.91 and 7.92 for the WCR and SSR sample respectively. Table 3 gives some value of dielectric parameters in several frequencies. The tandelta value in the table refers to the ratio of lossless dielectric to dielectric constant.

The log of imaginary part of permittivity (ϵ'') vs. log of frequencies (ω) is shown in Figure 5(b), form a straight line with negative slope. The slopes are -0.654 and -0.7333 for sample of WCR and SSR respectively, indicates that the conduction in SSR sample more predominantly dc conduction than that in WCR sample. The deviation of the slope from unity could be caused by effect of space charge at low frequency range[16,17].

The conductivity pattern for the Li_3PO_4 samples prepared by Wet Chemical and Solid State Reactions is shown at Figure 6. It can be observed that both of the ac conductivity increase with increasing frequency. Both samples make same slope of conductivity pattern in the high frequency area with slope for the WCR sample take


Figure 6. Frequency dependent plot of conductivity for Li_3PO_4 prepared by wet chemical reaction and solid state reaction.

a bit lower value than that for SSR indicates that WCR sample more dielectric and consequently more resistive than SSR sample.

At the lower frequency ($\log \omega = 3,5 - 6,8$), the conductivity patterns of WCR sample make another slope different from pattern for SSR sample. The conductivity is lower than the first slope, indicated that the resistance is bigger than the first one. This phenomenon give evidence to the Impedance Nyquist Plot that give two semicircle for WCR sample, where the grain boundary resistance value of second loop is bigger than the bulk resistance value of first loop as seen in Table 4.

Table 4. Comparison of parameters obtained from fit the experimental data to Jonscher power law $\sigma(\omega) = \sigma_0 + A\omega^s$ for every conductivity slope in Figure 6.

	WCR		SSR	
	Loop1	Loop2	total	total
$\log \omega$	2,5 – 3,5	3,5-6,8	2,5-6,8	2,5-6,8
σ_0 (S/cm)	5.17×10^{-10}	9.18×10^{-9}	6.43×10^{-9}	7.70×10^{-9}
A	4.78×10^{-10}	2.66×10^{-11}	4.06×10^{-11}	2.55×10^{-10}
s	0.3615	0.5503	0.5280	0.3961

Conductivity value of the samples was calculated from approximation of experimental conductivity plot to the Jonscher power Law:

$$\sigma(\omega) = \sigma_0 + A\omega^s \quad (2)$$

where $\sigma(\omega)$, σ_0 , A and s are referred to total conductivity, dc conductivity, ac conductivity constant and ac conductivity power respectively.

The conductivity parameters for WCR and SSR samples are shown in Table 4. Total conductivity of SSR sample is slight bigger than that for WCR, 7.70×10^{-9} S/cm and 6.43×10^{-9} S/cm respectively. But if we consider the grain boundary effect of WCR sample, the dc conductivity of SSR sample is in one order bigger than 5.17×10^{-10} S/cm of WCR. It seem like an anomaly because of WCR sample has better purity, more homogenous and smaller particle size which could lead to greater conductivity of the sample. The only thing was not owned by WCR sample is $\text{Li}_4\text{P}_2\text{O}_7$ phase. From this point of view we can conclude that the difference value of dc conductivity of WCR and SSR may be caused by the presence of $\text{Li}_4\text{P}_2\text{O}_7$ crystals in the solid state reaction sample that lead to a greater value.

CONCLUSION

We have synthesized Li_3PO_4 by two methods of preparation that is Solid State Reaction Method and Wet Chemical Reaction Method as a comparator method for the first one. The Wet Chemical Reaction Method is easier to do compared to Solid State Reaction one because of the absence of heating process in the preparation. In addition, WCR method could give more samples in one preparation than SSR method. Both of XRD spectra of WCR and SSR method were a

combination of crystalline and amorphous spectra, but WCR method give Li_3PO_4 phase more homogenous than SSR method which give impurity phase of $\text{Li}_4\text{P}_2\text{O}_7$. The SEM micrographs and EDS quantitative analysis give countenance results to XRD spectra. The Impedance Spectra Diagram gave difference pattern for WCR and SSR samples. The difference may be caused by the different capacitive response of WCR sample in the low frequency range. Both of the preparation methods produce Li_3PO_4 powders which have same dielectric characteristic. At frequency 10 kHz, the dielectric constants were 7.91 and 7.92 for the WCR and SSR sample respectively. The conductivity plot for the samples has same patterns in higher frequency range. In lower frequency range the conductivity pattern for WCR sample has a different slope of conductivity may be caused by grain boundary response to the field. The dc conductivity of SSR sample is one order higher than of WCR that is 7.70×10^{-9} and 5.17×10^{-10} S/cm. The difference value of dc conductivity may be caused by the presence of $\text{Li}_4\text{P}_2\text{O}_7$ crystals in the SSR sample.

ACKNOWLEDGMENT

This work is funded by Indonesian Ministry of Research, Technology and Higher Education of The Republic of Indonesia. Thanks to our colleagues at The PSTBM-BATAN and them from Department of Metallurgy and Materials Engineering, Universitas Indonesia, for their support, discussions and contributions on this work.

REFERENCES

- [1]. G. Sahu, Z. Lin, J. Li, Z. Liu, N. Dudney, and C. Liang. "Air-Stable, High-Conduction Solid Electrolytes of Arsenic-Substituted Li_4SnS_4 ". *Energy Environ. Sci.*, vol. 7, no. 3, pp. 1053-1058, 2014.
- [2]. A. Hayashi, K. Noi, A. Sakuda, and M. Tatsumisago, "Superionic Glass-Ceramic Electrolytes for Room-Temperature Rechargeable Sodium Batteries". *Nat Commun*, vol. 3, pp. 856, 2012.
- [3]. J. W. Fergus. "Ceramic and Polymeric Solid Electrolytes for Lithium-ion Batteries". *J. Power Sources*, vol. 195, no. 15, pp. 4554-4569, 2010.
- [4]. E. Quartarone and P. Mustarelli. "Electrolytes for Solid-State Lithium Rechargeable Batteries: Recent Advances and Perspectives". *Chem. Soc. Rev.*, vol. 40, no. 5, pp. 2525-2540, 2011.
- [5]. E. Kartini, M. Nakamura, M. Arai, Y. Inamura, K. Nakajima, T. Maksum, W. Honggowiranto, and T. Y. S. P. Putra. "Structure and Dynamics of Solid Electrolyte $(\text{LiI})_{0.3}(\text{LiPO}_3)_{0.7}$ ". *Solid State Ionics*, vol. 262, pp. 833-836, 2014.
- [6]. E. Kartini, W. Honggowiranto, H. Jodi, Supardi, Wahyudianingsih and A. K. Jahya. "Synthesis and Characterization of New Solid Electrolyte Layer $(\text{Li}_2\text{O})_x(\text{P}_2\text{O}_5)_y$ ". in 14th Asian conference on Solid State Ionics, vol. 2, pp. 163-173, 2014.
- [7]. L. Popoviciu, B. Manoun, D. de Waal, M. K. Nieuwoudt, and J. D. Comins. "Raman Spectroscopic Study of Phase Transitions in Li_3PO_4 ". *J. Raman Spectrosc.*, vol. 34, no. 1, pp. 77-83, 2003.
- [8]. N. A. W. Holzwarth, N. D. Lepley, and Y. A. Du. "Computer Modeling of Lithium Phosphate and Thiophosphate Electrolyte Materials". *J. Power Sources*, vol. 196, no. 16, pp. 6870-6876, 2011.
- [9]. N. D. Lepley and N. A. W. Holzwarth. "Computer Modeling of Crystalline Electrolytes: Lithium Thiophosphates and Phosphates". *J. Electrochem. Soc.*, vol. 159, no. 5, pp. A538-A547, 2012.
- [10]. N. D. Lepley, N. A. W. Holzwarth, and Y. A. Du. "Structures, Li^+ Mobilities, and Interfacial Properties of Solid Electrolytes Li_3PS_4 and Li_3PO_4 from First Principles". *Phys. Rev. B*, vol. 88, no. 10, p. 104103, 2013.
- [11]. L. Dwi Prayogi, M. Faisal, E. Kartini, W. Honggowiranto, and Supardi. "Morphology and Conductivity Study of Solid Electrolyte Li_3PO_4 ". in AIP Conference Proceedings 1710, 030047 (2016), 2016.
- [12]. A. Nur I. P., E. Kartini, L. Dwi Prayogi, M. Faisal, and Supardi. "Crystal Structure Analysis of Li_3PO_4 Powder Prepared by Wet Chemical Reaction and Solid State Reaction by Using X-Ray Diffraction (XRD)". *Ionics, Int. J. Ionics Sci. Technol. Ion. Motion*, vol. 22, no. 7, pp. 1051-1057, 2016.
- [13]. A. K. Jahja, T. Y. S. P. Putra, H. Mugirahardjo, Supardi, A. Insani, and E. Kartini. "Analisis Struktural Bahan Elektrolit $(\text{Li}_2\text{O})_x(\text{P}_2\text{O}_5)_y$ ($x=5, y=1$) dengan Metoda Difraksi Neutron Resolusi Tinggi". in Prosiding Seminar Nasional Hamburan Neutron dan Sinar-X, 2015, pp. 23-31.
- [14]. V. I. Voronin, E. A. Sherstobitova, V. A. Blatov, and G. S. Shekhtman. "Lithium-Cation Conductivity and Crystal Structure of Lithium Diphosphate". *J. Solid State Chem.*, vol. 211, pp. 170-175, Mar. 2014.
- [15]. V.T. Kumar, A. S. Chary, S. Bhardwaj, A. M. Awasthi, and S. N. Reddy. "Dielectric Relaxation, Ionic Conduction and Complex Impedance Studies on NaNO_3 Fast Ion Conductor". *Int. J. Mater. Sci. Appl.*, vol. 2, no. 6, pp. 173-178, 2013.
- [16]. K. V. Babu, L. S. Devi, V. Veeraiah, and K. Anand. "Structural and Dielectric Studies of LiNiPO_4 and $\text{LiNi}_{0.5}\text{Co}_{0.5}\text{PO}_4$ Cathode Materials for Lithium-ion Batteries". *J. Asian Ceram. Soc.*, vol. 4, no. 3, pp. 269-276, Sep. 2016.
- [17]. G. T. Xavier, B. Thirumalairaj, and M. Jaganathan. "Effect of Piperidin-4-ones on the Corrosion Inhibition of Mild Steel in 1 N H_2SO_4 ". *Int. J. Corros.*, vol. 2015, p. 1-15, 2015.